STEM CELLS®

TRANSLATIONAL AND CLINICAL RESEARCH

Implantation Site and Lesion Topology Determine Efficacy of a Human Neural Stem Cell Line in a Rat Model of Chronic Stroke

EDWARD J. SMITH,[a,b] R. PAUL STROEMER,[b] NATALIA GORENKOVA,[a] MITSUKO NAKAJIMA,[a] WILLIAM R. CRUM,[c] ELLEN TANG,[b] LARA STEVANATO,[b] JOHN D. SINDEN,[b] MICHEL MODO[a,d]

[a]Department of Neuroscience, [c]Department of Neuroimaging, King's College London, Institute of Psychiatry, London, United Kingdom; [b]ReNeuron Ltd., Guildford, United Kingdom; [d]Department of Radiology, McGowan Centre for Regenerative Medicine, University of Pittsburgh, Pittsburgh, Pennsylvania, USA

Key Words. Stem cell transplantation • Neural stem cell • Stroke • Nervous system

ABSTRACT

Stroke remains one of the most promising targets for cell therapy. Thorough preclinical efficacy testing of human neural stem cell (hNSC) lines in a rat model of stroke (transient middle cerebral artery occlusion) is, however, required for translation into a clinical setting. Magnetic resonance imaging (MRI) here confirmed stroke damage and allowed the targeted injection of 450,000 hNSCs (CTX0E03) into peri-infarct tissue, rather than the lesion cyst. Intraparenchymal cell implants improved sensorimotor dysfunctions (bilateral asymmetry test) and motor deficits (footfault test and rotameter). Importantly, analyses based on lesion topology (striatal vs. striatal + cortical damage) revealed a more significant improvement in animals with a stroke confined to the striatum. However, no improvement in learning and memory (water maze) was evident. An intracerebroventricular injection of cells did not result in any improvement. MRI-based lesion, striatal and cortical volumes were unchanged in treated animals compared to those with stroke that received an intraparenchymal injection of suspension vehicle. Grafted cells only survived after intraparenchymal injection with a striatal + cortical topology resulting in better graft survival (16,026 cells) than in animals with smaller striatal lesions (2,374 cells). Almost 20% of cells differentiated into glial fibrillary acidic protein+ astrocytes, but <2% turned into FOX3+ neurons. These results indicate that CTX0E03 implants robustly recover behavioral dysfunction over a 3-month time frame and that this effect is specific to their site of implantation. Lesion topology is potentially an important factor in the recovery, with a stroke confined to the striatum showing a better outcome compared to a larger area of damage. STEM CELLS *2012;30:785–796*

Disclosure of potential conflicts of interest is found at the end of this article.

INTRODUCTION

Stroke affects 795,000 Americans each year, with an estimated cost of $73.7 billion [1]. Although it remains the main cause of adult disability in industrialized nations, little progress has been achieved to improve persisting impairments. Stem cell therapy is gradually emerging as a viable treatment for stroke in preclinical studies, but clinical translation remains a challenge [2, 3]. Ideally for the routine treatment of stroke, a homogenous stem cell product, scaled up and tested appropriately, should be available to guarantee a robust availability [4]. Human neural stem cell (hNSC) lines fit these criteria and potentially present an efficient paradigm for cell therapy.

Ample preclinical evidence is available that both animal and human neural stem cells are efficacious in preclinical models of stroke [5, 6]. One promising source of hNSCs is the CTX0E03 cell line that improves sensorimotor recovery in a dose-dependent manner [7, 8]. This cell line is of clinical grade and Good Manufacturing Process cell banks have been generated using a standardized manufacturing process [9]. In contrast to reports of hNSC migration [5], this cell line, however, only disperses within the vicinity from the site of injection [7].

Different injection sites provide specific microenvironments that can influence implantation efficacy. A chronic lesion cyst is filled with extracellular fluid, but lacks an extracellular matrix that would provide a structural support for cells to integrate. Apart from major blood vessels that survived the ischemic insult, microvascular blood supply is nonexistent within the poststroke cavity. The intracerebroventricular (ICV) environment is not too dissimilar to the lesion environment. Cerebrospinal fluid (CSF) is present throughout, but no blood supply or structural support is available. However, CSF being distributed throughout the brain can provide

Authors contributions: E.J.S.: collection and/or assembly of data, data analysis and interpretation, manuscript writing, and administrative support; R.P.S.: conception and design, collection and/or assembly of data, data analysis and interpretation, and manuscript writing; N.G., M.N., W.R.C., E.T., and L.S.: collection and/or assembly of data, data analysis and interpretation, and manuscript writing; J.D.S.: conception and design, financial support, data analysis and interpretation, and manuscript writing; and M.M.: conception and design, financial support, data analysis and interpretation, manuscript writing, and final approval of manuscript.

Correspondence: Michel Modo, Ph.D., University of Pittsburgh, McGowan Institute for Regenerative Medicine, 3025 East Carson Street, Pittsburgh, Pennsylvania 15203, USA. Telephone: 412-383-7200; Fax: (412) 647-0878; e-mail: modomm@upmc.edu Received November 10, 2011; accepted for publication December 12, 2011; first published online in STEM CELLS *EXPRESS* December 29, 2011. 1066-5099/2011/$30.00/0 doi: 10.1002/stem.1024

a channel for the distribution of injected cells. This delivery method has been shown to be an efficient means to distribute cells during embryo development and the early postnatal period [10]. By contrast, the peri-infarct environment provides an extracellular matrix and has an increased vasculature, although some neuronal loss and gliosis are also present. However, the distribution of cells to a larger area is more challenging, unless the cells are migrating to these affected areas, as is the case with mouse NSCs [6]. The potential distribution of cells via the CSF and the peri-infarct environment hence provides two contrasting microenvironments for injections that are of clinical relevance, but with potentially different outcomes [6].

It is also important to consider that stroke lesions differ in their topology and this is known to be an important factor in recovery [11, 12]. Because of the trajectory of the middle cerebral artery (MCA), striatal areas are invariably affected by occlusion, whereas cortical damage is more variable. There is increasing evidence that this regional topology is due to a collateral circulation in cortical tissue [13]. Although, previous clinical trials using NT2 cells have focused on circumscribed basal ganglia strokes [14], preclinical animal studies have mostly ignored lesion topology. Using serial noninvasive magnetic resonance imaging (MRI), the striatal and striatal + cortical lesion topology can, nevertheless, be reliably stratified. It is, thus, possible to determine how this affects efficacy.

We therefore here investigated if the efficacy of the CTX0E03 hNSCs is dependent on their implantation site and stroke lesion topology. Correlations between behavioral recovery and MRI-based anatomical changes, as well as cell survival and differentiation were also investigated. These results establish certain conditions that can affect the therapeutic efficacy of CTX0E03 hNSCs.

Experimental Procedures

Animals

All procedures were in accordance with the UK Animals (Scientific) Procedures Act 1986 and the ethical review process of King's College London. Sprague-Dawley rats (Harlan, U.K.) were acclimatized for at least 1 week prior to surgery. The following groups were included: normal animals to provide a continuous baseline of behavior and brain growth ($n = 16$), animals with middle cerebral artery occlusion (MCAo) + vehicle to establish the impact of stroke and implantation surgery ($n = 14$), MCAo + intraparenchymal (Par) implantation of stem cells to evaluate the efficacy of grafting into the peri-infarct area ($n = 13$), and MCAo + ICV injection ($n = 15$). Animals were randomly allocated to treatment groups using a sequence of random numbers after exclusion criteria were applied to exclude animals that did not have an ischemic lesion (Supporting Information Table S1, Fig. S1 summarizes the a priori power calculation). Figure 1 summarizes the experimental schedule. Experimenters were blinded to the treatment conditions of the animals during testing. For data analysis, experimenters were aware of the animals' groupings, but not treatments.

Middle Cerebral Artery Occlusion

Animals weighing between 280 and 330 g were randomly allocated either for sham or 60 minutes of right transient MCAo surgery, as previously described [15].

Magnetic Resonance Imaging

Acquisition. ^{1}H MRI was performed using a 7T MRI scanner (Varian). Animals were anesthetized with isoflurane (4% induction, 2% maintenance) in a mixture of O_2/N_2O (30:70). MR image acquisition consisted of a fast spin echo sequence (TR = 3,000 ms, ETL = 4, ESP = 15, effective TE = 60 ms, $k_0 = 4$, averages = 10, matrix = 128 × 128, FOV = 3 cm × 3 cm, number of slices = 45, slice thickness = 0.6 mm, in plane resolution = 0.234 mm × 0.234 mm, and time = 16 minutes). The volume of the whole brain, lesion, striatum, cerebral cortex, hippocampus, and lateral ventricles were measured using a manual segmentation method [16, 17]. To account for lesion topology, experimental groups were further divided into two subgroups consisting of those animals with an infarction restricted to the striatum versus those that have a larger damage that affects both the striatum plus cortex (Supporting Information Table S2).

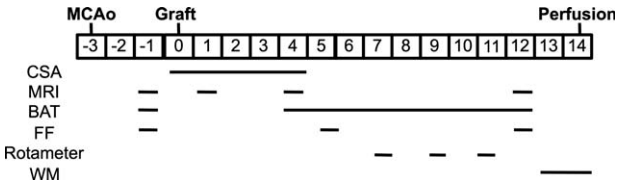

Figure 1. Experimental design and schedule. MCAo was induced 14 days prior to implantation. Animals were selected based on MRI 10 days following MCAo, with follow-up scans at 1, 4, and 12 weeks. Behavioral assessment consisted of the BAT, the FF, rotameter, and WM. CSA was administered from 1-day prior to 4 weeks after grafting. After all in vivo assessments were completed, animals were perfusion fixed prior to immunohistochemistry. Abbreviations: BAT, bilateral asymmetry test; CSA, cyclosporine A; FF, footfault test; MCAo, middle cerebral artery occlusion; MRI, magnetic resonance imaging; and WM, water maze.

Deformation-Based Morphometry. Deformation-based morphometry (DBM), as described in Vernon et al. [18], was used to identify common patterns of lesion enhancement and subtler morphological remodeling in the stroke compared with normal animals. The DBM analysis was performed at each time point using the normal group to account for ageing effects.

Behavioral Assessment

Establishing the efficacy of neural stem cells to recover behavioral dysfunctions in an animal model of stroke requires evaluation of these deficits on a variety of tests that reflect damage to sensorimotor, motor, and cognitive systems.

Bilateral Asymmetry Test. The bilateral asymmetry test is a test of tactile extinction probing sensory neglect [15]. Two strips of brown tape of equal size (6 cm long, 0.5-0.8 cm wide) were applied with equal pressure to the saphenous part of the forepaws. Two trials (300-second each) recorded the time to contact and removal for each paw. Sensorimotor bias was determined by subtracting the unaffected (right) from the affected (left) paw.

Footfault. The footfault test measures the animals' ability to integrate motor responses [19]. The rats were placed onto a suspended mesh wire (40 × 150 cm, 50 cm high, mesh size 5 cm) and the correct and incorrect placements (foot faults) of the affected forelimb are recorded over 60 seconds per trial (four trials per session).

Rotameter. Amphetamine-induced rotation (contralateral/ipsilateral) is used as an index of striatal damage. Lesioned and control animals were harnessed into jackets tethered to an

automated rotameter system (TSE Systems) and injected with amphetamine (2.5 mg/kg dissolved in 0.9% saline, i.p., Sigma) 30 minutes prior to assessment. The numbers of complete contralateral and ipsilateral rotations were then measured over 30 minutes.

Water Maze. The water maze (HVS) assesses spatial learning as a measure of cognitive deficits [20]. Rats were placed in a pool of water (2 m diameter, 21°C) with a submerged escape platform (10 cm diameter, 2 cm below water surface). Animals were trained for five consecutive days (two trials per day, 60-second) with the time to find the platform being recorded as evidence of spatial learning. At the end of the learning paradigm, a probe trial (60-second) measured the animals' memory of the platform position with percentage of time spend in each quadrant and annulus reflecting a memory of the platform location. In a separate trial (60-second max), the time taken to swim to a visible platform was assessed to control for potential motor deficits.

Cell Implantation

Cell Preparation. Derivation, culturing, and characterization of the cmyc-ER^{TAM} conditional immortal CTX0E03 human neural stem cell line is described in Pollock et al. [7]. Supporting Information Table S3 summarizes the chemically defined media to grow these cells. For implantation, CTX0E03 cells (P32-36) from frozen Drug Substance Lot vials were revived and seeded on laminin-coated (mouse, 10 μg/ml, Trevigen) T175 flasks at a density of 5×10^6 cells in 35 ml of media for 4 days (>80% confluence). Cell suspensions were prepared by detaching cells from the flasks using TrypZean/EDTA (Lonza) and formulated in Hypothermisol (BioLife Solutions) at a concentration of 50,000 cells per microliter. Viability of this formulation was >90% prior to implantation and >81% after completion of the procedure.

Implantation. Under isoflurane anesthesia (4% induction, 2% maintenance), animals with intraparenchymal grafts received two deposits of a 4.5-μl cell suspension (in total 450,000 cells per rat, 1 μl/minute) at the following coordinates: 1, AP −1.3 mm; *L* −3.5 mm; *V* −6.5; 2, AP −1.8 mm; *L* −4.0 mm; *V* −6.0 mm). If the implantation site was damaged, coordinates were adjusted to the peri-infarct region (three animals). Animals with ICV grafts received a single injection of 9 μl of cell suspension (AP +0.8 mm; *L* −1.5 mm; *V* −4.5 mm).

Immunosuppression. Anti-inflammatory treatment was given daily using Solu-medrol (s.c., 20 mg/kg day 1-7; 10 mg/kg day 8-12; 5 mg/kg day 13-14, Pharmacia Upjohn). Immunosuppression was given for 14 days from the day of implantation for alternate days with cyclosporine A (s.c., Sandimmun, Novartis, 10 mg/kg) diluted in Chremophor EL (Sigma).

Histological Assessments

Animals were perfusion fixed with 0.9% NaCl and 4% Parafix (Pioneer). Brains were cut in 50 μm coronal sections directly onto microscope slides.

Stereology of Implanted Cell Survival. Sections were washed with phosphate-buffered saline (PBS) prior to incubation for 30 minutes in 0.3% H_2O_2 in methanol to quench endogenous peroxide activity. Nonspecific binding was blocked by a 1-hour incubation in 10% normal goat serum and 0.3% Triton X-100 in PBS. The mouse anti-human nuclear antigen antibody (1:400, MAB1218, Millipore) was incubated overnight at 4°C prior to incubation in a secondary biotinylated anitbody for 2 hours at RT followed by a 1-hour incubation in an avidin-biotinylated-peroxide complex (1:100, Vector). 3,3′-Diaminobenzidine (Sigma) was used as the chromagen. For stereology, the area occupied by grafted cells was manually delineated at ×2.5 before a sampling grid of 100 μm × 80 μm was applied (StereoInvestigator, Microbrightfield) with a counting frame of 50 μm × 30 μm. The optical fractionator method [21] was applied to estimate total cell number (coefficient of error ≤ 0.5) on every fifth section.

Cell Differentiation. The phenotypic fate of implanted cells (mouse-SC101, 1:200; Stem Cells) was established by immunohistochemistry for astrocytes (chicken anti-glial fibrillary acidic protein [anti-GFAP], 1:2,000, ab4674, Abcam) and neurons (rabbit anti-Fox3, 1:500, ab104225, Abcam). Appropriate secondary Alexa fluorescent dyes (Molecular Probes) were used to establish if transplanted cells were colabeled to indicate phenotypic differentiation. Cells were counted from five random sample sites in three adjacent sections.

Collagen IV Expression. Collagen IV is a marker of the basement membrane of vasculature that not only is damaged in stroke but also increases when new blood vessels are formed. It therefore provides a more general assessment of the status of the functional vasculature compared to markers for endothelial cells [22, 23]. For this, images (using a fixed exposure) were obtained from five fields-of-view within the striatum, cerebral cortex, and corpus callosum of each hemisphere. Intensity of expression was measured using an automated script recording average pixel intensity. Corpus callosum measurements were used to normalize the data.

Subependymal Zone Measurements. To capture a cumulative effect of subependymal zone (SEZ) activity, the thickness of the SEZ was measured based on 4′,6-diamindino-2-phenylindole (DAPI) staining in the contralateral and ipsilateral hemisphere using ×20 overlapping and stitched images. Incorporation of nucleotide analogs into SEZ dividing cells would only capture the presence of transient amplifying cells over a small period of time and potentially also be incorporated into dying cells [24]. The length of the SEZ was also measured to account for a potential increase of this area in an enlarged ventricle as this could affect the overall neurogenic output. SEZ thickness and length were quantified for slices corresponding to the middle of the lesion cavity (−0.5 mm Bregma), as well as 1 mm anterior and posterior to this slice.

Alu-polymerase chain reaction (PCR) of Graft Survival

Genomic DNA was extracted using the QIAamp DNA FFPE tissue kit (Qiagen). An average of 250 ng of genomic DNA was amplified using specific primers (forward TGAGG CAGGCGAATCGCTTGAA, reverse GACGGAGTTTCGCTC TTGTTG) and a fluorescein amidite (FAM)-labeled fluorogenic probe (CGCGATCTCGGCTCACTGCAACCTCCATCG; PrimerDesign) against a conserved region of the human Alu-Sq sequence (Accession number U14573). Quantification of the human CTX0E03 DNA in rat tissue was based on a standard curve (10-fold serial dilutions of cell equivalents) prepared using extracted gDNA from CTX0E03. Each standard was diluted in a background of 250 ng of rat gDNA. Cell equivalents of human gDNA were calculated assuming 6.6 pg of gDNA per CTX0E03.

Statistical Analysis

An a priori power analysis was performed using G*Power 3 (University of Trier), all other statistical tests were performed

using SPSS20 for Mac (IBM). Serial in vivo data were analyzed using a repeated measures or two-way analysis of variance (ANOVA) followed by a Bonferroni post hoc analysis. Independent *t* tests were calculated for density, volume, and distance of surviving cells, whereas survival, collagen IV, and SEZ measurements were compared with one-way ANOVAs followed by a Bonferroni post hoc analysis. Pearson's correlations and multiple regressions were used to determine associations between independent data sets. All data are expressed as means ± standard error of means.

RESULTS

Efficacy of CTX0E03 Depends on Implantation Site and Lesion Topology

Sensorimotor function of the contralateral (left) forepaw was severely affected by MCAo with an increased time to remove tape from the affected paw (Fig. 2: Supporting Information Table S4 summarizes the main statistical effects; Supporting Information Table S5 summarizes post hoc comparisons). Only the peri-infarct intraparenchymal injection of CTX0E03 resulted in a gradual improvement of function between 4 and 10 weeks postimplantation. There was no further improvement after 10 weeks postimplantation. ICV implanted animals were indistinguishable from those receiving an intraparenchymal injection of suspension vehicle. Lesion topology indicated that rats with stroke damage confined to the striatum recovered this dysfunction to control levels following striatal CTX0E03 cell implantation. Animals with striatal lesions showed a more substantial improvement (83%) with CTX0E03 cell implantation, compared to animals with striatal and cortical lesions (48% improvement).

This therapeutic efficacy of cell implantation was further evident on motor tasks, where an intraparenchymal injection significantly improved motor coordination on the footfault test. Although there was no evidence of recovery at 4 weeks, there was a significant improvement at 12 weeks postimplantation. Again, the striatal lesion group exhibited less of a deficit compared to the larger striatal + cortical lesion group. However, intraparenchymal grafts exhibited a comparable recovery in both lesion types. A reduction in rotational asymmetry due to amphetamine injection further corroborated this improvement in motor function. ICV grafts did not improve either of these measures. An intraparenchymal implantation of cells therefore improves motor function, but lesion topology does not significantly affect this graft-mediated recovery.

To probe cognitive (learning and memory) dysfunction, rats were trained to find a submerged platform in the water maze. There was a significant learning impairment in acquisition after stroke and this was consistent for both lesion topologies. There was also no improvement in memory performance on the probe trial, although animals with striatal lesions and ICV grafts remembered the platform location as well as controls. To ensure that these deficits were not due to the stroke animals' motor deficits, their swim speed to a visible platform was also recorded and indicated that the stroke animals consistently swam faster than controls. Cell implantation therefore did not improve the cognitive deficits evident after stroke.

Cell Implantation Does Not Affect Evolution of Damage

MR images were acquired preimplantation, as well as 1, 4, and 12 weeks postimplantation (Fig. 3A). Importantly, the lesion topology from individual animals demonstrates that two subgroups of lesion topology were present after MCAo. One lesion topology only affected the striatal region, whereas a second more severe lesion involved striatal and cortical regions (Fig. 3B). The additional damage to the cortex also translated into a larger lesion volume in this subgroup (Fig. 3C). Neither intraparenchymal nor ICV implantation affected lesion volume or its evolution over time. Implantation of CTX0E03 also did not impact on the atrophy of the striatum or cortex. Measuring an entire anatomical region is, however, relatively insensitive to small local effects. A more refined analysis of subtle local effects based on deformation-based morphometry revealed a clear distinction of control animals compared to the three stroke groups (Fig. 3D). Nevertheless, implantation of CTX0E03 did not result in any changes that were statistically significant even at the voxel level (Fig. 3E). These results therefore indicate that hNSC implantation did not result in any detectable macroscopic changes in brain anatomy after stroke.

Although no gross anatomical changes were evident after cell implantation on MR images, a linear regression indicated that the volume of the ipsilateral striatum is a sufficient predictor of outcome on the bilateral asymmetry test ($F = 7.123$, $R^2 = 0.313$, $p < .001$), the footfault test ($F = 18.062$, $R^2 = 0.546$, $p < .001$) and the rotameter ($F = 7.513$, $R^2 = 0.542$, $p < .001$). Although cortical volumes were also associated with these deficits, they did not significantly add to the predictive power of the ipsilateral striatum. None of the serial MRI measures was a significant predictor of learning in the water maze. Therefore, changes in the striatum are related to behavioral outcome after stroke, but they are insufficient to indicate therapeutic efficacy.

Only Intraparenchymal Grafts Survive

A microscopic evaluation indicated that CTX0E03 cells survived after intraparenchymal implantation (Fig. 4A), but not after ICV implantation. Stereological cell counts revealed a mean graft survival of 10,337 ± 3,077 cells. However, in striatal + cortical lesions 6.75 times more cells survived (16,026 cells) compared to striatal ones (2,374 cells, Fig. 4B). Two animals did not have any surviving cells. These results were further corroborated by Alu-PCR (Fig. 4C). Although cell density in the grafts was comparable between both lesion topologies (Fig. 4D), the volume of striatal + cortical grafts was 4.2 times greater (Fig. 4E). This larger graft volume was due to the dispersion of cells along the anterior-posterior axis (Fig. 4F). These surviving CTX0E03 cells integrated into the rat tissue (Fig. 4G) with 20.63% ± 2.23% differentiating into GFAP+ astrocytes (Fig. 4H). However, only in striatal + cortical lesions did implanted cells produce FOX3-positive neurons (2%, Fig. 4I).

There was no association between the number of surviving cells and behavioral outcome. However, the spread (dispersion) of the graft significantly correlated with performance on the bilateral asymmetry test ($r = 0.463$, $p < .05$) and footfault test ($r = 0.340$, $p < .05$). Lesion volume was associated with the spread ($r = 0.86$, $p < .001$) and the volume of implanted cells ($r = 0.492$, $p < .01$), with striatal lesions having a smaller spread and volume. The amount of remaining striatal tissue was, however, not associated with graft survival or spread. Instead, implanted cells dispersed more if there was less cortical tissue ($r = -0.557$, $p < .01$). Differentiation into astrocytes was dependent on lesion size ($r = 0.813$, $p < .01$) with more cells differentiating into astrocytes if there was less striatum ($r = -0.712$, $p < .01$) or cortex ($r = -0.732$, $p < .01$) remaining. Cell survival ($r = 0.544$, $p <$

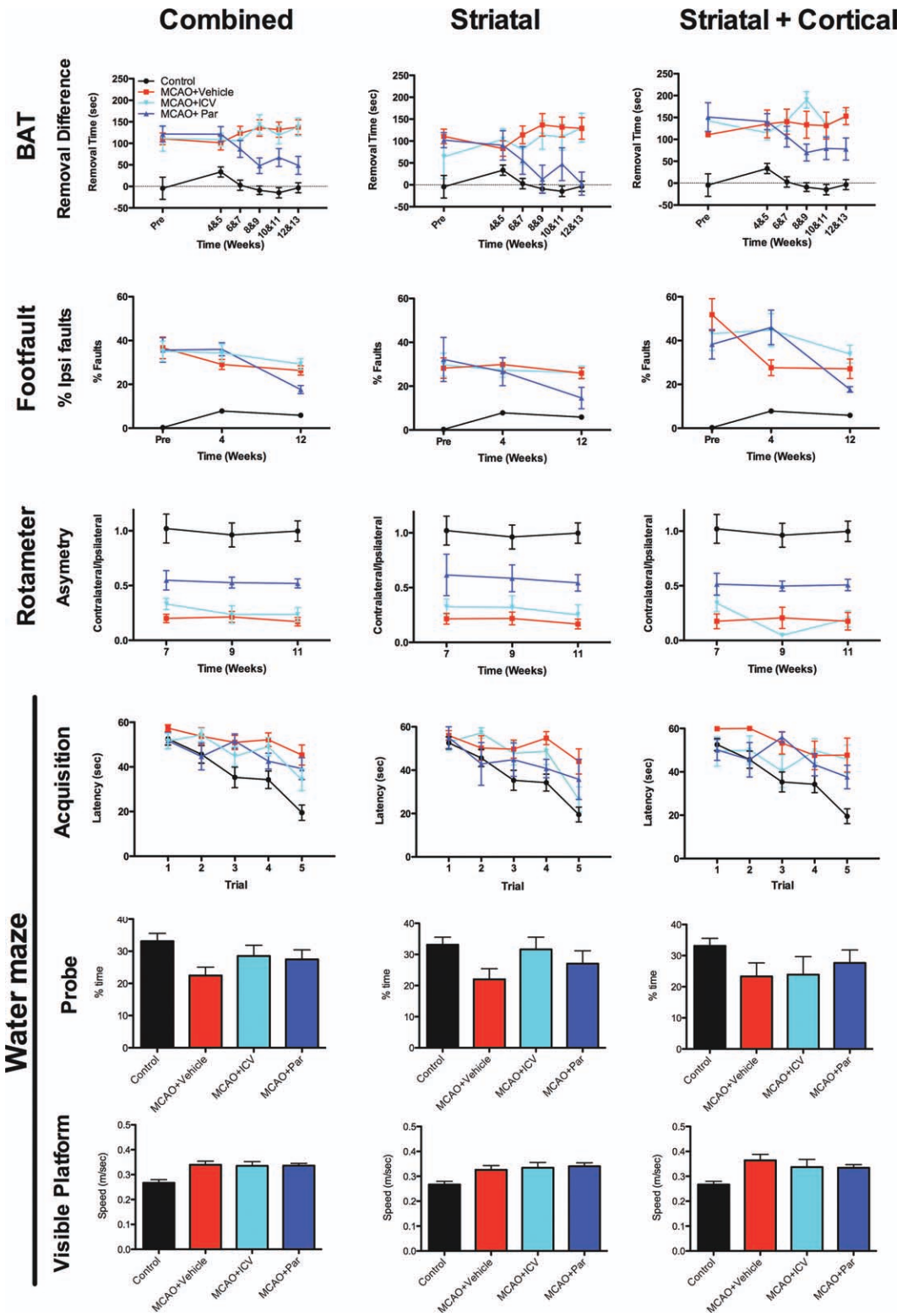

Figure 2. Behavioral assessment. Rats with MCAo damage exhibited a consistent behavioral deficit on the BAT, the footfault test, the rotameter (amphetamine-induced rotations), as well as the water maze. To determine whether topology of the lesion affects the type or severity of deficits, MCAo animals were subgrouped into those animals with a lesion confined to the striatum (striatal group) and those that exhibited a large area of damage that encompassed the striatum and cortex. An intraparenchymal implantation of cells (MCAo + Par) improved performance on the BAT, footfault, and rotameter test. However, the deficit in the water maze was unaffected. ICV injection of cells did not produce any improvements. Location of implantation is therefore essential to ensure a consistent behavioral recovery. Abbreviations: BAT, bilateral asymmetry test; ICV, intracerebroventricular; MCAo, middle cerebral artery occlusion; and Par, intraparenchymal.

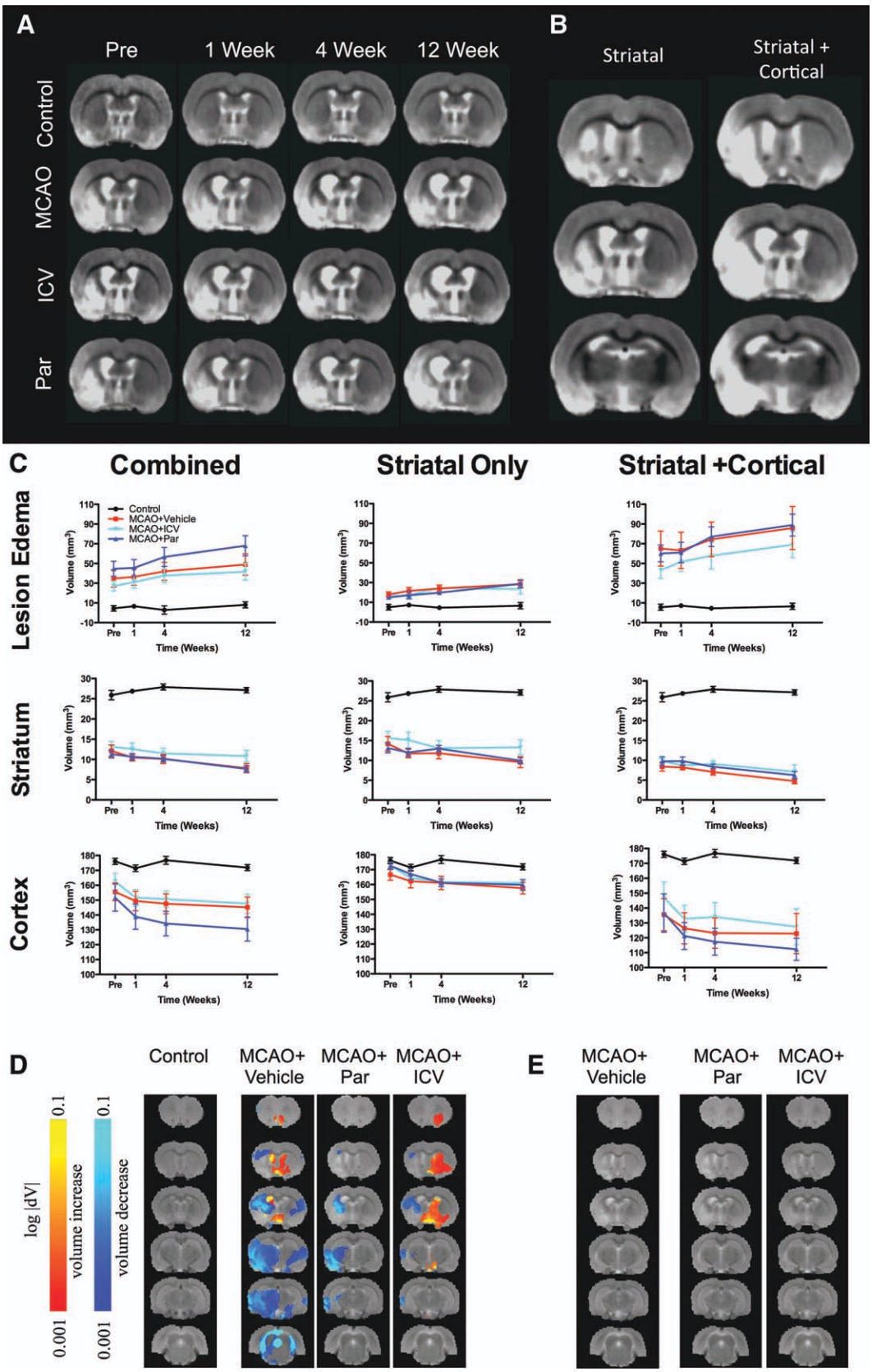

Figure 3. Magnetic resonance imaging (MRI). **(A):** Overview of MR images for each group over time. MR images were coregistered and averaged to provide a group mean for each experimental condition. **(B):** Mean group images of striatal, as well as striatal + cortical stroke lesion. **(C):** Measurement of region of interest (ROIs) consisting of the lesion (edema-corrected), ipsilateral striatum, and cortex revealed no significant difference between experimental groups. **(D):** As ROIs only look at large structures and might not be sensitive enough to detect small local changes potentially relevant to recovery, a deformation-based morphometry analysis was calculated. Prior to implantation, MCAo groups revealed a significant shrinkage of tissue in the lesion area (cold voxels), but also areas of expansion (hot voxels), such as the ipsilateral ventricle compared to normal control animals. **(E):** Although clear differences can be detected between all MCAo groups when compared with controls, a direct comparison of treated versus the MCAo + vehicle group revealed no significant changes at the voxel level. This lack of difference between the treated and MCAo + vehicle group was consistent over time indicating that even at the voxel level no significant effects of the implanted cells could be detected. Abbreviations: ICV, intracerebroventricular; MCAo, middle cerebral artery occlusion; and Par, intraparenchymal.

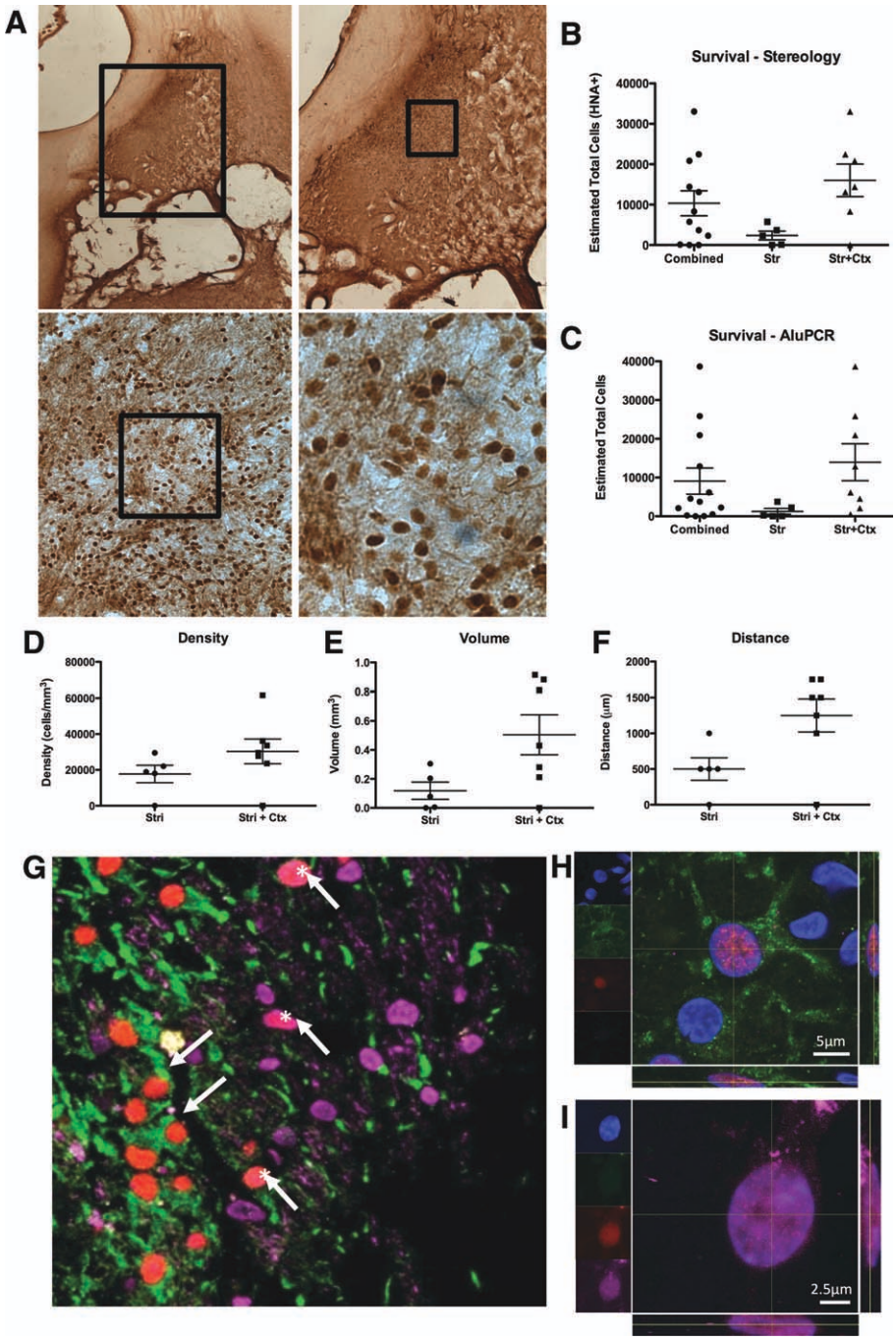

Figure 4. Cell survival and differentiation. **(A):** Bright-field image of implanted CTX0E03 (using a human nuclear antibody) in the stroke-damaged striatum. **(B):** A stereological assessment of human cells in the rat striatum indicated an overall variable survival of implanted cells. Survival was largely dependent on lesion topology. Implantation into Str + Ctx lesions resulted in a better survival of cells compared to those confined to the striatum (Str; $t = 2.775$, $p < .01$). **(C):** This same group difference was also evident if cell survival was corroborated using qAlu-PCR. **(D):** However, there was no difference in the density of implanted cells within the grafts. **(E):** The better cell survival in the Str + Ctx lesions was a reflection of a larger graft volume. **(F):** This increased volume was mainly a consequence of a wider spread of cells in the anterior-posterior axis in the Str + Ctx grafts. **(G):** Implanted cells (SC101 in red) in the Str + Ctx group differentiated into both neurons (Fox3 in Pink, * indicates neuronal differentiation) and astrocytes (glial fibrillary acidic protein [GFAP] in green). Higher magnification confocal images of these cells reveal a colocalization of SC101 with GFAP **(H)** and FOX3 **(I)**. In the Str lesions, implanted cells only differentiated into astrocytes, but not neurons. Abbreviations: Ctx, cortical; HNA, human nuclei antigen; PCR, polymerase chain reaction; Str, striatum.

.05) and graft volume ($r = 0.577$, $p < .05$) were also important factor in astrocytic differentiation. Importantly, astrocytic differentiation also translated in an association with behavioral performance on the bilateral asymmetry test ($r = 0.499$, $p < .01$), the footfault test ($r = 0.366$, $p < .01$), and the rotameter ($r = -0.455$, $p < .01$). Astrocytic differentiation therefore is an important factor that is relevant to behavioral improvements.

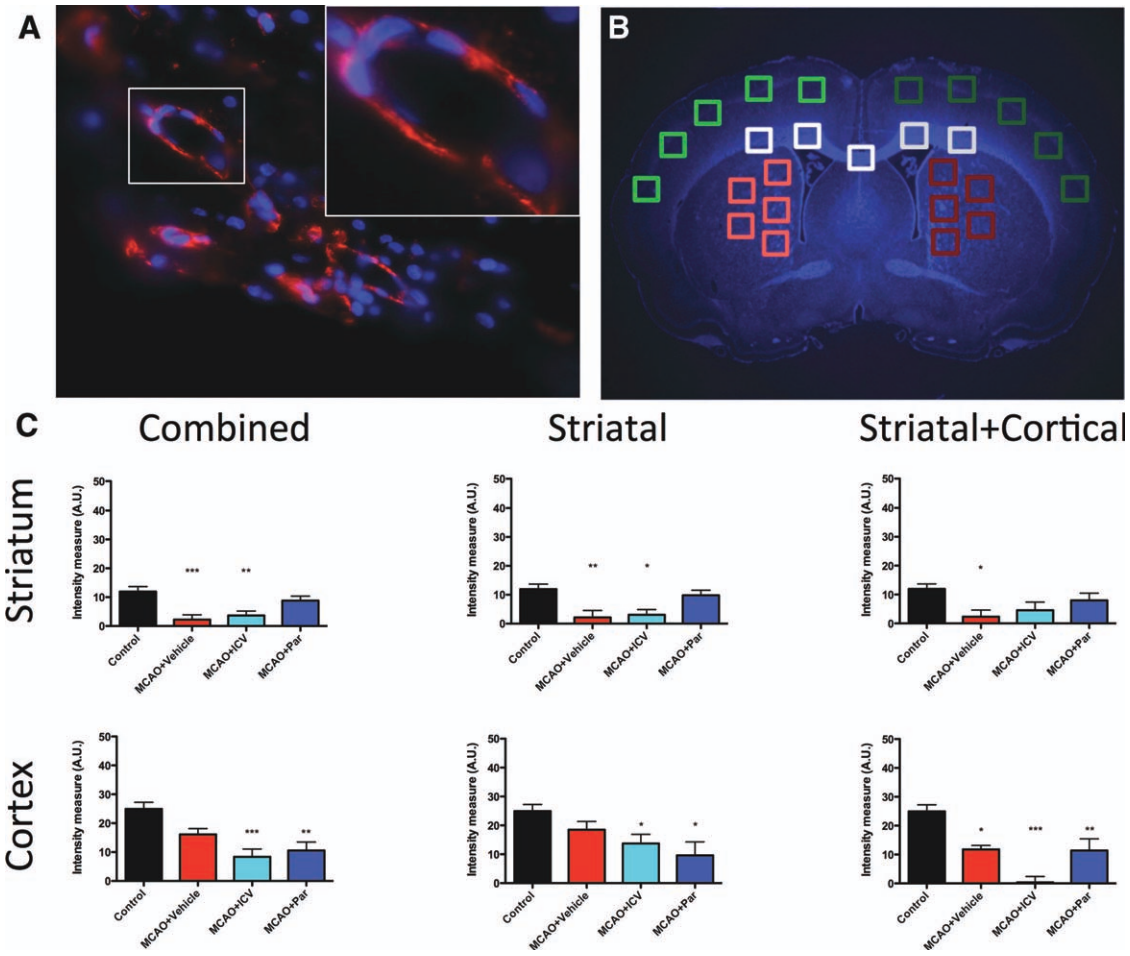

Figure 5. Collagen IV expression. **(A):** Collagen IV is expressed in the basement membrane of blood vessels. **(B):** Fluorescence intensity of collagen IV was measured in ipsilateral and contralateral regions of interest consisting of striatum and cortex. Measurements of collagen IV intensity of the corpus callosum served as an internal standard to allow comparison between animals. **(C):** Collagen IV expression was increased outside the glial scar in the striatum after an intraparenchymal implantation of CTX0E03 compared to MCAo + vehicle. This increased expression was therefore due to the implanted cells rather than the surgical trauma. This increased presence of collagen IV in the MCAo + Par group was comparable to normal controls. However, in the ipsilateral cortex implantation of cells did not increase expression of collagen IV. Abbreviations: ICV, intracerebroventricular; MCAo, middle cerebral artery occlusion; and Par, intraparenchymal. *<.05; **<.01; ***<.001.

Intraparenchymal Grafts Impact on Host Vasculature

Stroke affects not only the neuropil but also endothelial cells within the neurovascular niche. A restoration of the basement membrane of damaged blood vessels, as well as an increase in blood vessels, was reflected by an increase in collagen IV expression (Fig. 5A). Collagen IV levels in the peri-infarct striatal area (Fig. 5B) were significantly decreased after stroke (Fig. 5C). This was consistent in both lesion topologies. An intraparenchymal injection of CTX0E03 restores collagen IV to almost control levels. By contrast, an ICV cell implantation had no impact on collagen IV levels. In animals with striatal stroke, where damage did not extend to the cortex, no change in collagen IV levels was evident in the cortex, whereas in those lesions where stroke damage extended to the cortex, a significant decrease in collagen IV was evident. Surprisingly, an ICV injection of CTX0E03 further reduced the level of collagen IV in this lesion topology.

Collagen IV expression was dependent on the size of the lesion ($r = 0.443$, $p < .001$), as well as spared striatal ($r = -0.276$, $p < .05$) and cortical tissue ($r = -0.441$, $p < .001$). The differentiation of implanted cells into astrocytes was also associated with striatal collagen IV ($r = 0.299$, $p < .01$) as is the performance of the footfault ($r = 0.247$, $p < .05$). None of the other behavioral measures were correlated with collagen IV. These associations indicated that the vasculature is potentially an important factor in promoting recovery.

Implantation of CTX0E03 Did Not Affect Endogenous Neurogenesis

The stroke cavity did not extend to the SEZ, where endogenous neurogenesis generates a constant flux of new neurons that can potentially influence recovery. However, the lateral ventricle was enlarged (Fig. 6A) due to changes in the peri-infarct region with patches of gliosis and large areas of neuronal loss (Fig. 6B). Structural alterations within the SEZ impact on the rostral migratory stream and immature neurons that infiltrate surrounding striatal tissue (Fig. 6C). This structural alteration was evident in the thickness of the dorsal part of the subependymal zone (Fig. 6D). Ventrally, however, gliosis (Fig. 6E) leads to an almost complete loss of the SEZ

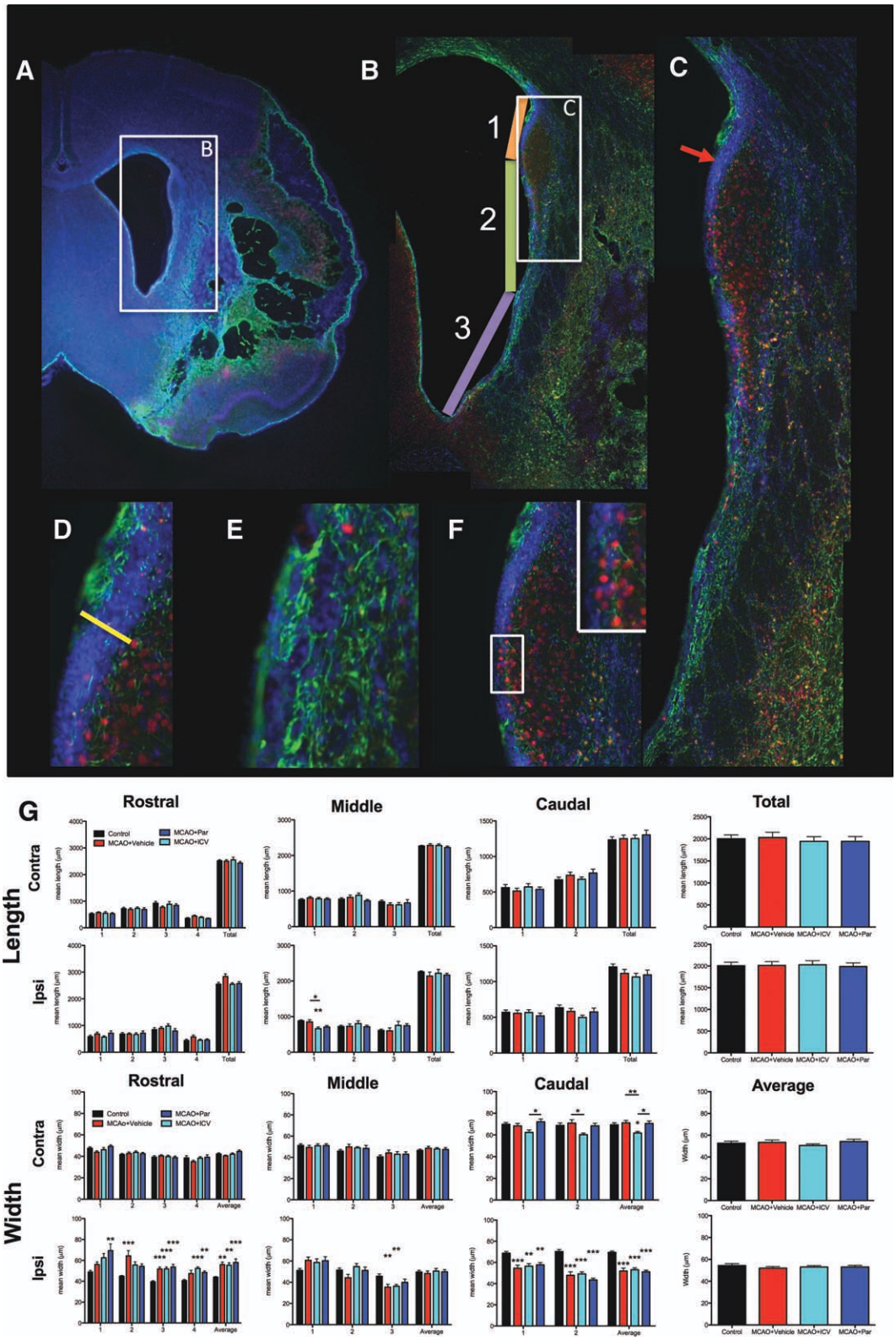

Figure 6. Endogenous neurogenesis. The damage caused by stroke affects striatal architecture and can extend to the subependymal zone **(A)**. The subependymal zone (SEZ) elongates along the rostral-caudal axis and is composed of three segments that each has a distinct length **(B)**. Apart from these elements, the thickness of the SEZ varies along the dorsal-ventral axis **(C)**. Measurement of this thickness is related to the total number of cells (DAPI) in the SEZ **(D)**. However, other qualitative difference can also be observed, such as glial scarring (glial fibrillary acidic protein in green) of the lesion environment disrupting the SEZ **(E)**, or neuronal cells (Fox3 in red) in an area with an apparent lack of a SEZ **(F)**. Quantification of the length and width of the SEZ **(G)** indicated that stroke damage increased the width of the SEZ in the rostral part, but a decrease was present in the caudal part. This resulted in no overall increased in SEZ width if all these measurements are taken together. Implanted cells did not significantly impact on any of these measurements compared to MCAo + vehicle. The length of the SEZ (and hence ventricle) was not significantly affected by stroke or implantation. Abbreviations: DAPI, 4′,6-diamindino-2-phenylindole; ICV, intracerebroventricular; MCAo, middle cerebral artery occlusion; and Par, intraparenchymal.

(Fig. 6E). As the ventricles were enlarged after stroke, the overall length of the SEZ could have influenced its overall neurogenesis potential. However, there was no significant change in SEZ length after stroke or cell grafting (Fig. 6G). An enlargement of the ventricles was therefore due to changes in its width rather than length. By contrast, the thickness of the SEZ was significantly altered. The rostral part of the lesion exhibited a thicker SEZ throughout compared to control animals (Fig. 6G). In the middle of the lesion, however, there was no dramatic change in thickness, whereas in the caudal part of the lesion there was actually a decrease in the SEZ. These opposing changes were negatively correlated with each other ($r = -0.501$, $p < .001$) indicating that as the caudal SEZ decreased, the rostral SEZ enlarged.

These changes in SEZ width of the rostral and caudal sections were influenced by lesion volume ($r = 0.293$, $p < .05$; $r = -0.384$, $p < .01$), striatal ($r = -0.637$, $p < .001$; $r = 0.685$, $p < .001$), cortical ($r = -0.320$, $p < .01$; $r = 0.397$, $p < .01$) and ventricular size ($r = 0.567$, $p < .01$; $r = -0.695$, $p < .001$). Linear regressions indicated that ipsilateral striatum was the best predictor of the rostral SEZ changes ($F = 35.933$, $R^2 = 0.404$, $p < .001$), whereas caudal changes in the SEZ were mostly due to the size of the ipsilateral ventricle ($F = 48.154$, $R^2 = 0.476$, $p < .001$). Although these SEZ changes were also associated with performance on the bilateral asymmetry test ($r = 0.318$, $p < .01$; $r = -0.306$, $p < .01$), the footfault test ($r = 0.451$, $p < .001$; $r = -0.545$, $p < .001$) and rotameter ($r = -0.482$, $p < .001$; $r = 0.526$, $p < .001$), these associations were likely to be due to stroke damage affecting the SEZ and behavior in a similar fashion. Although cell implantation did not significantly alter the SEZ, changes in the SEZ were associated with the density of the graft ($r = 0.711$, $p < .01$; $r = -0.576$, $p < .05$) and astrocytic differentiation ($r = 0.388$, $p < .05$; $r = -0.434$, $p < .001$), but these associations were also likely to be due to stroke damage influencing these parameters in a similar fashion rather than any direct causal effects.

Discussion

Stem cell administration for stroke is emerging as a promising therapeutic strategy. Using a battery of behavioral tests, serial MRI, and post-mortem histology, we here determined that the CTX0E03 cell line is efficacious in a rat model of stroke if injected into the peri-infarct area. A stroke confined to the striatum benefited most from this therapeutic intervention. Implantation sites, as well as lesion topology, are hence important factors that influence the efficacy of hNSC in stroke.

Therapeutic Efficacy

Therapeutic efficacy in stroke is determined by improvements in behavioral dysfunctions, as these will be the main comparators in patients. There is a clear relationship between the size of the lesion and the degree of impairment in preclinical models of stroke [25], but the nature of the deficits is dependent on anatomical location. Larger lesions affecting multiple brain regions (i.e., striatum + cortex) therefore produce a more significant impairment. It is, nevertheless, fundamental to recognize that even a stroke restricted to the striatum affects multiple functional systems (sensorimotor, motor, cognitive, and emotional). A comprehensive behavioral assessment is needed to measure the dysfunction and recovery of as many functional systems as possible. Failing to measure dysfunction/recovery on one of the systems might lead to a false negative, whereas focusing on just one system might produce an overestimation of the overall potential therapeutic efficacy. In the context of translational studies, it is important to note that some basic motor functions can recover spontaneously and potentially are easily recovered in rodents [26]. More complex and persistent behavioral deficits are likely to be a better reflection of chronic deficits found in human patients. We therefore used a battery of behavioral tests that are largely resistant to spontaneous recovery in the rat [15, 16].

A persistent deficit was evident in sensorimotor functions as measured by the bilateral asymmetry test, motor functions as assessed by the rotameter and footfault test, as well as cognitive functions measured by the water maze. A gradual and significant change in these deficits was evident between 4 and 8 weeks postimplantation, but no further improvements beyond this were observed. This is akin of the time course of recovery of mouse neural stem cells [6, 16] and primary human neural progenitor cells [27]. Only implantation into the intraparenchymal peri-infarct region significantly improved outcome. This type of damage and implantation is also the main focus for clinical studies [12, 14, 28]. A smaller lesion limited to a single anatomical structure is a more restricted damage that is easier to recover. Still, there was also an improved outcome in the larger striatal + cortical lesions, highlighting the potentially wider benefit of these cells in stroke. It remains unclear though if implantation of more cells into the larger lesions could achieve a similar recovery as that observed in the striatal lesion. The implantation microenvironment and lesion topology are therefore important factors to consider for cell therapy. The major challenge here remains the attribution of recovery on these different tasks to putative neurobiological mechanisms.

Mechanism(s) of Recovery

A variety of mechanisms can potentially promote recovery after stroke. Exogenous replacement of lost cells through survival and differentiation is often considered the predominant focus of cell therapy. Indeed, only animals with cell survival here showed recovery, but there was no correlation between the survival of implanted cells and degree of recovery. Instead, the dispersion of cells was associated with recovery and lesion size. The regional dispersion of these surviving cells is therefore an important factor that influences the recovery process. However, it remains unclear if the distribution of cells is the key factor to mediate recovery or if it is the presence of cells in particular peri-lesion locations that determines if animals recover or not. As surviving cells were confined to the striatum, this is the likely site of action of the cells, although they might mediate effects in other remote locations (e.g., thalamus and cortex). Still, the mechanism(s) of action is likely to be subtle and localized as serial MRI and deformation-based morphometry did not uncover any systematic structural effects on neuroanatomy. Recovery is therefore unlikely to be mediated through a significant neuroprotective effect.

The 2% of neuronal differentiation of hNSCs is also unlikely to be a key factor in animals' recovery, as these were only found in the larger lesions. In contrast to replacing lost neurons, hNSCs' astrocytic differentiation (20%) in both of these lesion types was associated with outcome and hence could play a major role in recovery. During the chronic phase of stroke, astrocytes can promote neuronal/synaptic plasticity through secretion of thrombospondin and angiogenesis through secretion of vascular endothelial growth factor and related proteins, as well as through

production of elements of the extracellular matrix, such as matrix metalloproteinases or collagens [29, 30]. Collagen IV here was upregulated in the peri-infarct area in the presence of implanted cells and was linked to the astrocytic differentiation of implanted cells. As collagen IV in this area was mostly associated with the basement membrane, it reflects the restoration of damaged vessels, as well as the formation of new blood vessels. Angiogenesis has been widely documented after cell implantation [31–33] and is known to be associated with astrocytes [34]. Although the formation of new blood vessels could explain the time gap between cell injection and recovery, it is unclear how "angiogenesis" relates to behavioral recovery. Therefore, these new blood vessels must exert an indirect effect on the neuropil. It is, however, also conceivable that angiogenesis is an epiphenomenon that is not relevant to behavioral recovery. Targeted loss-of-function experiments are required to establish and distinguish unequivocally which mechanism(s) is the cause of therapeutic efficacy.

Implications for Clinical Translation

Although understanding the mechanism of action is not a requirement to initiate clinical trials, as long as a robust therapeutic efficacy can be demonstrated [35], it is essential to improve and optimize cell therapy. If it can be unequivocally established that recovery is mediated through angiogenesis and/or the astrocytic differentiation of implanted cells, these processes can be specifically targeted to improve recovery. However, just being able to generate new blood vessels is unlikely to be sufficient to induce efficacy, but promoting these processes in the appropriate location is essential for a positive outcome. Presuming that the mechanisms these cells invoke will be the same in human patients as in animal models, it is therefore desirable to define the necessary and sufficient conditions under which implanted cells can promote an improvement in function. As indicated here an appropriate site of injection (peri-infarct) can determine if cells survive or not, hence providing a necessary condition for efficacy. By contrast, lesion topology provides a sufficient condition, as it affects the degree of recovery, but is not controlling if there is a benefit or not. Establishing a framework of appropriate conditions in preclinical animal models will therefore continue to contribute to the appropriate design of future trials aimed to assess efficacy [14, 28].

Conclusion

The implantation of hNSCs (CTX0E03) can improve behavioral impairments after stroke. However, this improvement is contingent on their appropriate placement. Lesion topology and size can significantly influence behavioral recovery, as well as the survival and differentiation of implanted cells. Differentiation of the grafted cells into an astrocytic phenotype is associated with the recovery of function along with the dispersion of cells within the peri-infarct striatum. This knowledge should aid in the design of clinical trials aiming to establish therapeutic efficacy in patients with stroke.

Acknowledgments

We acknowledge funding support from the NIBIB Quantum Grant program (1 P20 EB007076-01), the MRC Translational Stem Cell Initiative (G0800846), and ReNeuron Ltd. We thank Dr Ivan Rattray for helping in the blinding of the conditions of the animals.

Disclosure of Potential Conflicts of Interest

R.P.S., E.S., E.T., L.S., and J.S. are employees of ReNeuron Ltd. J.S. is a cofounder of ReNeuron Ltd. M.M. has received grant and personnel support from ReNeuron for this study.

References

1 Lloyd-Jones D, Adams RJ, Brown TM et al. Heart disease and stroke statistics—2010 update: A report from the American Heart Association. Circulation 2010;121:e46–e215.
2 Borlongan CV. Cell therapy for stroke: Remaining issues to address before embarking on clinical trials. Stroke 2009;40(3 suppl): S146–S148.
3 Chopp M, Steinberg GK, Kondziolka D et al. Who's in favor of translational cell therapy for stroke: STEPS forward please? Cell Transplant 2009;18:691–693.
4 Hodges H, Pollock K, Stroemer P et al. Making stem cell lines suitable for transplantation. Cell Transplant 2007;16:101–115.
5 Kelly S, Bliss TM, Shah AK et al. Transplanted human fetal neural stem cells survive, migrate, and differentiate in ischemic rat cerebral cortex. Proc Natl Acad Sci USA 2004;101:11839–11844.
6 Modo M, Stroemer RP, Tang E et al. Effects of implantation site of stem cell grafts on behavioral recovery from stroke damage. Stroke 2002;33:2270–2278.
7 Pollock K, Stroemer P, Patel S et al. A conditionally immortal clonal stem cell line from human cortical neuroepithelium for the treatment of ischemic stroke. Exp Neurol 2006;199:143–155.
8 Stroemer P, Patel S, Hope A et al. The neural stem cell line CTX0E03 promotes behavioral recovery and endogenous neurogenesis after experimental stroke in a dose-dependent fashion. Neurorehabil Neural Repair 2009;23:895–909.
9 Thomas RJ, Hope AD, Hourd P et al. Automated, serum-free production of CTX0E03: A therapeutic clinical grade human neural stem cell line. Biotechnol Lett 2009;31:1167–1172.
10 Campbell K, Olsson M, Bjorklund A. Regional incorporation and site-specific differentiation of striatal precursors transplanted to the embryonic forebrain ventricle. Neuron 1995;15:1259–1273.
11 Parkinson BR, Raymer A, Chang YL et al. Lesion characteristics related to treatment improvement in object and action naming for patients with chronic aphasia. Brain Lang 2009;110:61–70.
12 Feys H, Hetebrij J, Wilms G et al. Predicting arm recovery following stroke: Value of site of lesion. Acta Neurol Scand 2000;102:371–377.
13 Cheng B, Golsari A, Fiehler J et al. Dynamics of regional distribution of ischemic lesions in middle cerebral artery trunk occlusion relates to collateral circulation. J Cereb Blood Flow Metabol 2011; 31:36–40.
14 Kondziolka D, Steinberg GK, Cullen SB et al. Evaluation of surgical techniques for neuronal cell transplantation used in patients with stroke. Cell Transplant 2004;13:749–754.
15 Modo M, Stroemer RP, Tang E et al. Neurological sequelae and long-term behavioural assessment of rats with transient middle cerebral artery occlusion. J Neurosci Methods 2000;104:99–109.
16 Modo M, Beech JS, Meade TJ et al. A chronic 1 year assessment of MRI contrast agent-labelled neural stem cell transplants in stroke. Neuroimage 2009;47(suppl 2):T133–T142.
17 Ashioti M, Beech JS, Lowe AS et al. Neither in vivo MRI nor behavioural assessment indicate therapeutic efficacy for a novel 5HT(1A) agonist in rat models of ischaemic stroke. BMC Neurosci 2009;10:82.
18 Vernon AC, Crum WR, Johansson SM et al. Evolution of extra-nigral damage predicts behavioural deficits in a rat proteasome inhibitor model of Parkinson's disease. PLoS One 2011;6:e17269.
19 Hernandez TD, Schallert T. Seizures and recovery from experimental brain damage. Exp Neurol 1988;102:318–324.
20 Morris RG, Garrud P, Rawlins JN et al. Place navigation impaired in rats with hippocampal lesions. Nature 1982;297:681–683.

21 West MJ, Slomianka L, Gundersen HJ. Unbiased stereological estimation of the total number of neurons in the subdivisions of the rat hippocampus using the optical fractionator. Anat Rec 1991;231: 482–497.
22 Hamann GF, Schrock H, Burggraf D et al. Microvascular basal lamina damage after embolic stroke in the rat: Relationship to cerebral blood flow. J Cereb Blood Flow Metabol 2003;23: 1293–1297.
23 Franciosi S, De Gasperi R, Dickstein DL et al. Pepsin pretreatment allows collagen IV immunostaining of blood vessels in adult mouse brain. J Neurosci Methods 2007;163:76–82.
24 Ming GL, Song H. Adult neurogenesis in the mammalian central nervous system. Annu Rev Neurosci 2005;28:223–250.
25 Irle E. An analysis of the correlation of lesion size, localization and behavioral effects in 283 published studies of cortical and subcortical lesions in old-world monkeys. Brain Res: Brain Res Rev 1990;15: 181–213.
26 Markgraf CG, Green EJ, Watson B et al. Recovery of sensorimotor function after distal middle cerebral artery photothrombotic occlusion in rats. Stroke 1994;25:153–159.
27 Andres RH, Horie N, Slikker W et al. Human neural stem cells enhance structural plasticity and axonal transport in the ischaemic brain. Brain: J Neurol 2011;134(Pt 6):1777–1789.
28 Kalladka D, Muir KW. Stem cell therapy in stroke: Designing clinical trials. Neurochem Int 2011;59:367–370.
29 Ritz MF, Fluri F, Engelter ST et al. Cortical and putamen age-related changes in the microvessel density and astrocyte deficiency in spontaneously hypertensive and stroke-prone spontaneously hypertensive rats. Curr Neurovas Res 2009;6:279–287.
30 Milner R, Hung S, Wang X et al. Responses of endothelial cell and astrocyte matrix-integrin receptors to ischemia mimic those observed in the neurovascular unit. Stroke 2008;39:191–197.
31 Jiang Q, Zhang ZG, Ding GL et al. Investigation of neural progenitor cell induced angiogenesis after embolic stroke in rat using MRI. Neuroimage 2005;28:698–707.
32 Zhang P, Li J, Liu Y et al. Human embryonic neural stem cell transplantation increases subventricular zone cell proliferation and promotes peri-infarct angiogenesis after focal cerebral ischemia. Neuropathology 2011;31:384–391.
33 Horie N, Pereira MP, Niizuma K et al. Transplanted stem cell-secreted vascular endothelial growth factor effects poststroke recovery, inflammation, and vascular repair. Stem Cells 2011;29: 274–285.
34 Zhao Y, Rempe DA. Targeting astrocytes for stroke therapy. Neurotherapeutics 2010;7:439–451.
35 Savitz SI, Chopp M, Deans R et al. Stem cell therapy as an emerging paradigm for stroke (STEPS) II. Stroke 2011;42:825–829.


See www.StemCells.com for supporting information available online.